Robustness of networks against fluctuation-induced cascading failures

Dominik Heide,[1,*] Mirko Schäfer,[1,†] and Martin Greiner[2,‡]
[1]*Frankfurt Institute for Advanced Studies and Frankfurt International Graduate School for Science, Johann Wolfgang Goethe Universität, Ruth-Moufang-Straße 1, D-60438 Frankfurt am Main, Germany*
[2]*Corporate Technology, Information & Communications, Siemens AG, D-81730 München, Germany*
(Received 9 November 2007; published 8 May 2008)

Fluctuating fluxes on a complex network lead to load fluctuations at the vertices, which may cause them to become overloaded and to induce a cascading failure. A characterization of the one-point load fluctuations is presented, revealing their dependence on the nature of the flux fluctuations and on the underlying network structure. Based on these findings, an alternate robustness layout of the network is proposed. Taking load correlations between the vertices into account, an analytical prediction of the probability for the network to remain fully efficient is confirmed by simulations. Compared to previously proposed mean-flux layouts, the alternate layout comes with significantly less investment costs in the high-confidence limit.

DOI: 10.1103/PhysRevE.77.056103 PACS number(s): 89.75.Hc, 02.50.Fz, 89.75.Da

I. INTRODUCTION

Much of the infrastructure of modern societies is organized in complex networks. A failure may lead to dramatic consequences. It is important to understand the properties and vulnerabilities of these networks. Error and attack tolerance against random and intentional removal of vertices and links has already been widely studied [1–8]. Also dynamical failures have been discussed [9–15], where a component failure and a subsequent network-wide redistribution of loads might trigger further cascading failures.

A simple network model to describe a cascading failure has been put forward by [9]. Every vertex i of the network $G=(\mathcal{V},\mathcal{E})$, described by the sets of vertices $\mathcal{V}$ and edges $\mathcal{E}$, sends a unit flux $s_{if}=1$ to every other vertex $f\neq i$ along the shortest-hop paths $[i\rightarrow f]$. This results in an accumulated vertex load

$$L_v = \frac{1}{N(N-1)} \sum_{i,f\in\mathcal{V}} r_{sp}([i\rightarrow f];v)s_{if}. \tag{1}$$

The value of the path function $r_{sp}([i\rightarrow f];v)$ is either 1 or 0, depending on whether the vertex v is part of the shortest-hop path from vertex i to f or not [16]. Based on the load (1), the capacities

$$C_v(\alpha) = (1+\alpha)\langle L_v\rangle \tag{2}$$

are assigned to the vertices. If for some reason one or more vertices fail, a network-wide redistribution of the loads (1) occurs due to a modification of the shortest paths. The new load L_v of vertex v may become larger than its capacity C_v and subsequent failures can occur. This sequence of events is referred to as a cascading failure. In order to reduce or ideally prevent the occurrence of such cascading failures, other capacity layouts have been proposed [15,17] besides (2). So far, all of these approaches have one thing in common. They assume the flux matrix s_{if} to be uniform and constant. There are many interesting examples where this is not the case. In communication and transportation networks s_{if} is known as the traffic matrix which is subject to temporal fluctuations. Electricity networks with a large share of renewable power generation come with strongly fluctuating source fluxes. More fluctuations in electricity networks are introduced by power exchange markets.

There is a strong need to study the impact of fluctuating fluxes on the robustness of networks. Vertices may fail either directly due to an accumulation of extreme flux fluctuations or due to a subsequent overload cascade. Immediate questions that arise are: How does an efficient capacity layout look, which is able to cope with the fluctuating fluxes? Given various classes of fluctuating fluxes, how do they determine the resulting fluctuations in the accumulated vertex loads? Are there correlations between the accumulated loads of different vertices and how do they look? In the following we will give answers to these important questions.

II. LOAD FLUCTUATIONS RESULTING FROM FLUX FLUCTUATIONS

Flux fluctuations are introduced into the modeling (1) by varying the strengths s_{if} according to some distribution. For demonstration, we pick a lognormal distribution with mean $\langle s\rangle=1$. The fluctuation strength is defined as its standard deviation $\sigma=\sqrt{\langle(s-1)^2\rangle}$. We distinguish two fluctuation scenarios. The first is denoted as pathlike, where all s_{if} are drawn independently from each other. For the second, which we denote as sourcelike, all $s_{if}=s_i$ belonging to the same source vertex i are given the same value sampled from the lognormal distribution.

In order to develop a new capacity layout beyond the mean-flux case (2), a good understanding is needed on how the flux fluctuations determine the load distributions across the network. We begin by looking at the one-point distribution $p_v(L_v)$. Expression (1) can be read as a weighted sum of independently and identically distributed random fluxes s_{if}. In the case of lognormal fluxes with small fluctuation strengths $\sigma\lesssim 1$, this sum can be approximated again by a

*dheide@fias.uni-frankfurt.de
†schaefer@fias.uni-frankfurt.de
‡martin.greiner@siemens.com

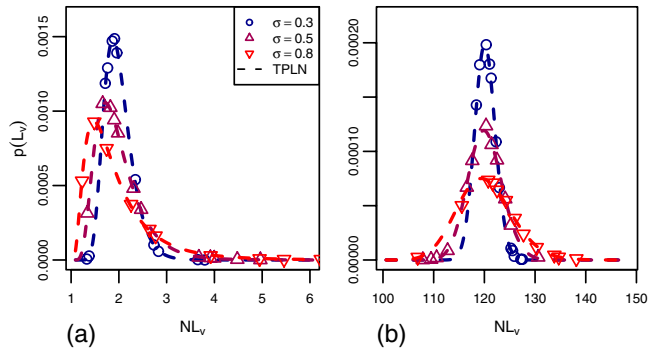

FIG. 1. (Color online) Simulated load distributions $p(L_v)$ due to sourcelike flux fluctuations for three fluctuation strengths. Two vertices with minimum (a) and maximum (b) load are depicted. One typical realization of a random scale-free network, for which the number of vertices, scale-free exponent, and minimum degree have been set to $N=1000$, $\gamma=2.5$ and $k_{\min}=2$, has been used with 10^4 fluctuation realizations. The dashed curves correspond to the three-parameter lognormal distribution (TPLN, 3) with predicted parameters (4) and (5).

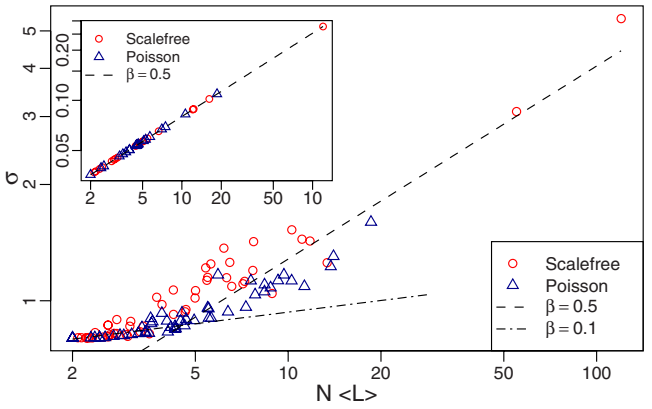

FIG. 2. (Color online) The moment $\sigma(L_v)=\sqrt{\langle L_v^2\rangle_c}$ of Eqs. (4) and (5) as a function of the average vertex load $\langle L_v\rangle$ for one realization of pathlike (inset) and sourcelike fluctuations on random scale-free (circles) and Poisson (triangles) networks. Parameters are $N=1000$, $\gamma=2.5$, $k_{\min}=2$ for the scale-free networks, and $N=1000$, $\langle k\rangle=5$ for the Poisson networks. Fifty out of 10^3 vertices are shown. The dashed and dashed-dotted straight lines represent the scaling exponents $\beta=0.5$ and 0.1.

lognormal distribution [18]. To allow for some more flexibility we choose a three-parameter generalization of the lognormal distribution

$$p_v(L_v) = \frac{1}{\sqrt{2\pi}\eta(L_v-\kappa_v)}\exp\left[-\frac{(\ln[L_v-\kappa_v]-\mu_v)^2}{2\eta_v^2}\right] \quad (3)$$

for the description of the load distribution. To fit the load distribution at vertex v, the three parameters μ_v,η_v,κ_v are calculated from the first three cumulants of Eq. (3) which have to be equal to the first three cumulants of the load (1). These are for pathlike fluxes

$$\langle L_v^n\rangle_c = \langle s^n\rangle_c \sum_{i\neq f=1}^{N}\left(\frac{r_{sp}([i\to f];v)}{N(N-1)}\right)^n, \quad (4)$$

and for sourcelike fluxes

$$\langle L_v^n\rangle_c = \langle s^n\rangle_c \sum_{i=1}^{N}\left(\sum_{f=1(f\neq i)}^{N}\frac{r_{sp}([i\to f];v)}{N(N-1)}\right)^n. \quad (5)$$

Figure 1 compares the predicted three-parameter lognormal distribution (3)–(5) with simulated one-point load distributions, which have been sampled from a large number of independent flux fluctuation realizations on a typical random scale-free network. For pathlike (not shown) as well as sourcelike flux fluctuations and for all vertices ranging from minimum to maximum average load, the analytical distributions fit the numerical data very well. Note that the one-point load distribution (3) needs not to be mixed up with the distribution $p(\langle L_v\rangle)$ of average loads across all vertices of the network. For the latter we reproduce the result $p(\langle L\rangle)\sim\langle L\rangle^{-\delta}$ with $\delta\approx 2.2$, which has been shown [19] to be universal for all scale-free networks with exponent $2<\gamma\leq 3$.

The $n=2$ cumulants of Eqs. (4) and (5) are depicted in Fig. 2 as a function of the averaged vertex loads. For pathlike flux fluctuation (inset in Fig. 2) a scaling relation of the type $\sqrt{\langle L_v^2\rangle_c}\sim\langle L_v\rangle^{\beta}$ is found with exponent $\beta=0.5$. This dispersion relation has already been observed in [20] and related to internal collective dynamics on the network. However, it has not been clear whether the found value of the scaling exponent is universal or not. For sourcelike flux fluctuations no good overall scaling is observed. This is due to the fact that only the load distribution for high average loads are Gaussian shaped, whereas load distributions of vertices with small loads have a long tail that increases the variance; consult again Fig. 1. The asymptotic high or low load regimes are in accordance with $\beta=0.5$ and 0.1, respectively, indicating that the scaling exponent $\beta\approx 0.5$ is not universal.

III. EFFICIENT CAPACITY LAYOUT

The good agreement of the predicted three-parameter lognormal distributions with the vertex loads allows for a direct construction of a new capacity layout, which is robust against the flux fluctuations up to some confidence level. For a single vertex the quantile

$$q = \int_0^{C_v} p_v(L_v)dL_v = F_v(C_v) \quad (6)$$

describes the confidence level that its load L_v remains smaller than its capacity C_v. Since $1-q$ describes the probability that the vertex will fail due to direct overloading, a confidence level very close to one is desirable. A typical value in engineering is $q=0.9999$. By presetting the confidence level to such a targeted value, the capacity $C_v(q)=F_v^{-1}(q)$ needed at the vertex is obtained from the inverse of the cumulative distribution function F_v. Since $p_v(L_v)$ is three-parameter lognormal, F_v can be expressed in terms of the inverse of the cumulative distribution function Φ of a centered normal distribution with unit variance. This leads to the capacity assignment

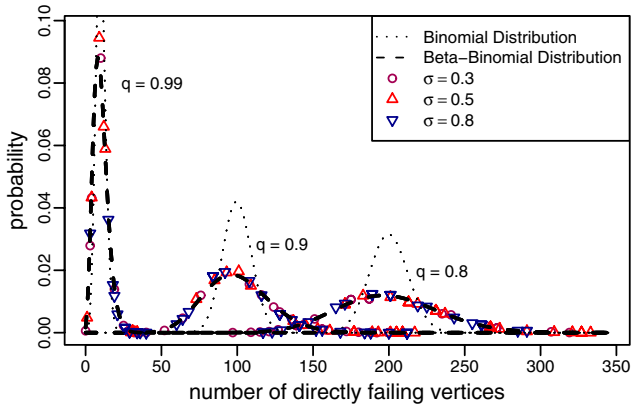

FIG. 3. (Color online) Probability distributions for the number of directly failing vertices due to sourcelike flux fluctuations in a scale-free network. Network parameters are as in the previous figures. 10^4 flux realizations have been used for various fluctuation strengths. The distributions only depend on the quantile (6): $q=0.8$ (right), 0.9 (center), and 0.99 (left). The dotted and dashed curves correspond to binomial and beta-binomial distributions with the same mean $(1-q)N$. The correlation parameter ρ of the beta-binomial distribution has been calculated with Eqs. (9) and (10).

$$C_v(q) = e^{\eta_v \Phi^{-1}(q)+\mu_v} + \kappa_v. \tag{7}$$

In principle, different q values could be assigned to different vertices, but for simplicity we chose the same q for all vertices.

By this construction, the distribution of the number of directly failing vertices M due to the fluctuating fluxes will have a mean of $\langle M\rangle=(1-q)N$. As can be seen in Fig. 3 the actual number may deviate much from this mean. Note that the shown distributions only depend on the quantile q and not on the strength of the flux fluctuations. The distributions would be binomial if the direct failure of a vertex were independent of the other vertices, however, this is not the case. The probabilities of directly failing vertices are correlated since all vertices on a shortest path receive the same flux strength from the transmitting vertex.

A good approximation to the observed distributions is provided by the beta-binomial distribution

$$p(M;a,b) = \binom{N}{M} \frac{B(M+a, N-M+b)}{B(a,b)}, \tag{8}$$

where $B(\cdot,\cdot)$ is the beta function. It is known to describe correlated Bernoulli random variables [21]. The two parameters a and b can be rewritten as the mean $\langle M\rangle/N=(1-q)=\frac{a}{a+b}$ and the correlation measure $\rho=\frac{1}{a+b+1}$. From best fits of Eq. (8) to the distributions of Fig. 3 we find the empirical relation

$$\rho = \omega_N (1-q)^{\xi}, \tag{9}$$

(see Fig. 4). Within acceptable precision the exponent ξ turns out to be independent of the network size. For ω_N the N dependence

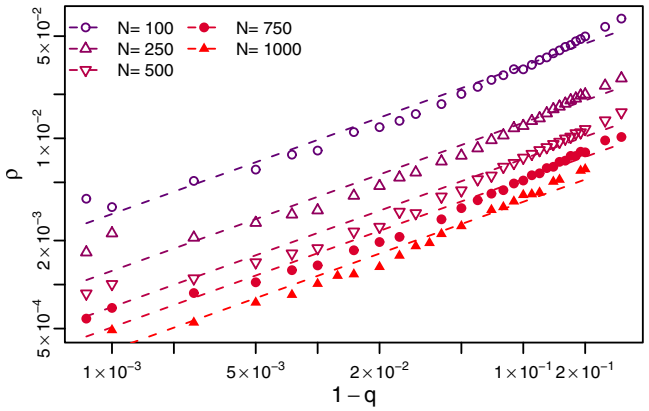

FIG. 4. (Color online) Relation between the parameters ρ and $(1-q)$ of the beta-binomial distributions (8), which have been directly fitted to the sampled distributions of Fig. 3.

$$\omega_N = \omega N^{-\nu} \tag{10}$$

is found. The following table lists the fitted parameter values for pathlike and sourcelike flux fluctuations on scale-free ($\gamma=2.5$, $k_{\min}=2$) as well as Poisson networks ($\langle k\rangle=5$).

Path	ω	ξ	ν	Source	ω	ξ	ν
Poisson	1.50	0.53	0.80	Poisson	5.40	0.70	0.80
Scale-free	1.47	0.41	0.80	Scale-free	3.34	0.51	0.80

The good description by the beta-binomial distribution (8) allows one to make an analytical prediction of the probability that with the capacity layout (7) no vertex of the network will fail due to flux fluctuations. This probability $p(M=0;1-q,\rho)$ with ρ from Eqs. (9) and (10) is equal to the probability that the network efficiency [6]

$$E = \frac{1}{N(N-1)} \sum_{i\neq f\in\mathcal{V}} \frac{1}{d_{if}} \tag{11}$$

remains equal to its initial value E_0 of the intact network, thus $p(\frac{E}{E_0}=1)=p(M=0;1-q,\rho)$. The network efficiency represents a measure to evaluate the quality of a capacity layout. It includes direct as well as cascading failure of vertices. d_{if} is the shortest-hop distance between vertices i and f. Figure 5 compares the predicted $p(M=0;1-q,\rho)$ with numerical data.

Since the correlation ρ of the beta-binomial distribution goes to zero as q goes to one, the probability $p(\frac{E}{E_0}=1)$ can also be approximated using the binomial distribution $p_{bin}(M=0;1-q)$; see again Fig. 5. This gives a parameter-free approximation to the probability that no vertex fails. The same relation also holds for pathlike flux fluctuations.

Finally, we compare the investment costs $I=\Sigma_{v\in\mathcal{V}}C_v=I(\alpha)=I(q)$ relative to $I_0=\Sigma_{v\in\mathcal{V}}\langle L_v\rangle$ of the two capacity layouts (2) and (7). These are functions of the tolerance parameter α and the quantile q, respectively. Figure 6 shows the efficiency (11) of a scale-free network as a function of I. For sourcelike flux fluctuations the efficiency of Eq. (7) remains close to zero up to a critical investment cost, only then to jump up and to overtake the efficiency of Eq. (2). In the limit

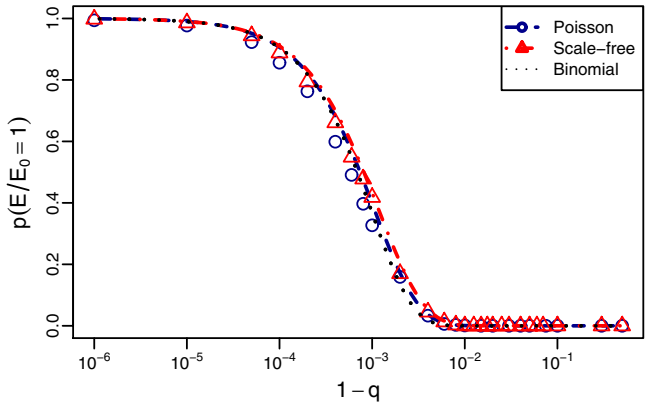

FIG. 5. (Color online) Probability for the relative efficiency to remain $\frac{E}{E_0}=1$ given the capacity layout (7) against sourcelike flux fluctuations. The symbols have been determined from a simulation of 10^3 fluctuation realizations with strength $\sigma=0.5$ on a representative random scale-free (triangles) and Poisson (circles) network of size $N=1000$ (other parameters as stated before). The dashed and dotted curves represent the analytical prediction based on the beta-binomial distribution (8) and the binomial simplification, respectively.

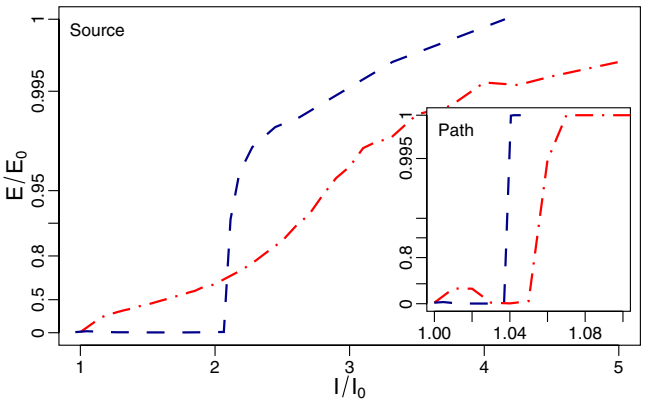

FIG. 6. (Color online) Relative efficiency of a typical $N=1000$ scale-free network as a function of investment costs against direct vertex failures as well as subsequent cascading failures induced by pathlike (inset) and sourcelike fluctuations of strength $\sigma=0.8$. Dashed-dotted and dashed curves represent the capacity layouts (2) and (7), respectively. All curves come with a confidence level of 0.99, meaning that 10 out of the simulated 10^3 fluctuation realizations result in relative efficiencies below the curve.

$E/E_0 \to 1$ the investment costs into the newly proposed capacity layout (7) are significantly smaller than for the standard layout (2). For pathlike flux fluctuations both capacity layouts reveal an abrupt transition from low to high efficiency at very low investment costs.

IV. CONCLUSION

A robust capacity layout has been developed. It is able to cope with the load fluctuations induced by flux fluctuations transported on the network. Within a given confidence level it supports the network to operate at full efficiency and guarantees robustness against a cascading failure. Since these findings have been based on a simple network model [9], it will make sense to discuss various model extensions, such as those proposed in Refs, [22–24], which distinguish between internal and external fluctuation dynamics. The ultimate challenge will be to carry over these ideas to real-life infrastructure networks such as, for example, electricity networks facing a growing fraction of fluctuating renewable energy sources.

ACKNOWLEDGMENTS

We gratefully acknowledge support by the Frankfurt Center for Scientific Computing and thank Jan Scholz and Clemens Hoffmann for valuable comments.

[1] R. Albert, H. Jeong, and A.-L. Barabási, Nature (London) **406**, 378 (2000).
[2] R. Cohen, K. Erez, D. ben-Avraham, and S. Havlin, Phys. Rev. Lett. **85**, 4626 (2000).
[3] D. S. Callaway, M. E. J. Newman, S. H. Strogatz, and D. J. Watts, Phys. Rev. Lett. **85**, 5468 (2000).
[4] R. Cohen, K. Erez, D. ben-Avraham, and S. Havlin, Phys. Rev. Lett. **86**, 3682 (2001).
[5] A. E. Motter, T. Nishikawa, and Y. C. Lai, Phys. Rev. E **66**, 065103(R) (2002).
[6] P. Crucitti, V. Latora, M. Marchiori, and A. Rapisarda, Physica A **320**, 622 (2003).
[7] R. Albert, I. Albert, and G. L. Nakarado, Phys. Rev. E **69**, 025103(R) (2004).
[8] L. K. Gallos, R. Cohen, P. Argyrakis, A. Bunde, and S. Havlin, Phys. Rev. Lett. **94**, 188701 (2005).
[9] A. E. Motter, and Y. C. Lai, Phys. Rev. E **66**, 065102(R) (2002).
[10] A. E. Motter, Phys. Rev. Lett. **93**, 098701 (2004).
[11] P. Crucitti, V. Latora, and M. Marchiori, Phys. Rev. E **69**, 045104(R) (2004)
[12] P. Crucitti, V. Latora, and M. Marchiori, Physica A **338**, 92 (2004).
[13] R. Kinney, P. Crucitti, R. Albert, and V. Latora, Eur. Phys. J. B **46**, 101 (2005).
[14] E. J. Lee, K. I. Goh, B. Kahng, and D. Kim, Phys. Rev. E **71**, 056108 (2005).
[15] M. Schäfer, J. Scholz, and M. Greiner, Phys. Rev. Lett. **96**, 108701 (2006).
[16] In the case of shortest-path degeneracy, the value of the path function is reduced by a factor depending on the degrees and depths of the respective branching points.
[17] P. Li, B. H. Wang, H. Sun, P. Gao, and T. Zhou, Eur. Phys. J. B **62**, 101 (2008).
[18] M. Romeo, V. Da Costa, and F. Bardou, Eur. Phys. J. B **32**, 513 (2003).
[19] K.-I. Goh, B. Kahng, and D. Kim, Phys. Rev. Lett. **87**, 278701 (2001).

[20] M. A. de Menezes and A.-L. Barabási, Phys. Rev. Lett. **92**, 028701 (2004).
[21] M. Hisakado and S. Kitsukawa, J. Phys. A **39**, 15365 (2006).
[22] A.-L. Barabási, M. A. de Menezes, S. Balensiefer, and J. Brockman, Eur. Phys. J. B **38**, 169 (2004).
[23] Z. Eisler, J. Kertész, S.-H. Yook, and A.-L. Barabási, Europhys. Lett. **69**, 664 (2005).
[24] S.-H. Yook and M. A. de Menezes, Europhys. Lett. **72**, 541 (2005).